Supporting Information

Porous core-shell structured MoO_2-Mo_2C@C electrocatalysts for pH-universal hydrogen evolution reaction

Xinglong Zhang[a,b], Tingxi Chen[c], Ning Lu[a], Feiyu Jian[a], Bin Zhu[a], Yanning Zhang[c,d *], Liang He[e], Hui Tang[a *]

[a] *Department of Materials and Energy, University of Electronic Science and Technology of China, Chengdu 611731, P. R. China*

[b] *Department of Materials Science, Fudan University, Shanghai 200438, P. R. China*

[c] *Institute of Fundamental and Frontier Sciences, University of Electronic Science and Technology of China, Chengdu 611731, China*

[d] *Key Laboratory of Quantum Physics and Photonic Quantum Information, Ministry of Education of China, University of Electronic Science and Technology of China, Chengdu 611731, China*

[e] *School of Mechanical Engineering, Sichuan University, Chengdu 610065, P. R. China*

Density functional calculations were carried out with the Vienna *ab initio* simulation package (VASP). The Perdew-Burke-Ernzerhof (PBE) function, under the generalized gradient approximation (GGA), was used to describe the exchange-correlation function. The cut-off energy was set to 500 eV, and all the atoms were relaxed by the conjugate gradient (CG) method until the maximum force of each atom was less than 0.02 eV/Å. A 2×2 supercell in the lateral plane was applied to calculate the formation energy of the defects. We used a 5×7×1 Monkhorst-Pack special *k*-point mesh for the primitive unit cell, with 56 atoms, and the single Γ point for the supercell with 224 atoms.

The formation energy of defects is calculated to understand the transformation from MoO_2 (011) to Mo_2C (100) during heat preservation, which is defined as follows.

$$E_f = (E_{def} - E_{pris} \pm nE_i)/n,$$

Where E_{pris} and E_{def} represent the total energies of the pristine slab and the supercell with defects, respectively, n is the number of defects and E_i is the atomic energy of constituent i. The atomic energies of a single C atom in graphite and an O atom in CO_2 were used here as energy references.

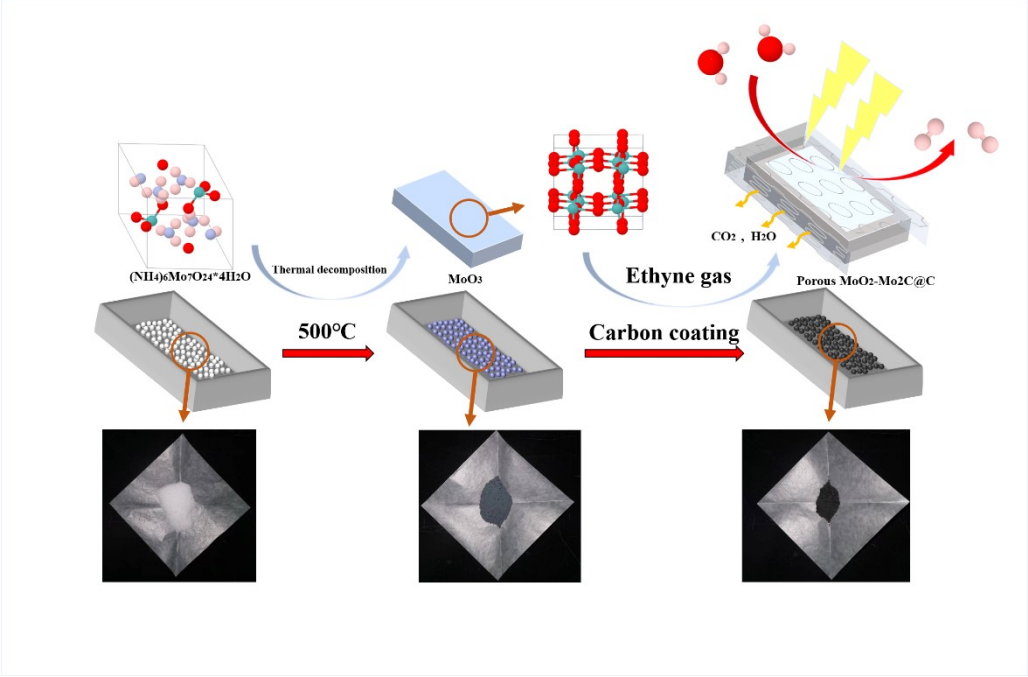

FigureS1. Schematic illustration of synthesis procedure of MoO_2-Mo_2C@C catalysts

The synthetic procedure of MoO_2-Mo_2C@C is schematically displayed in the graphic abstract. The MoO_3 nanoflake was first synthesized through a thermal decomposition method. After that, the porous core-shell MoO_2-Mo_2C@C was fabricated by a carbon coating process.

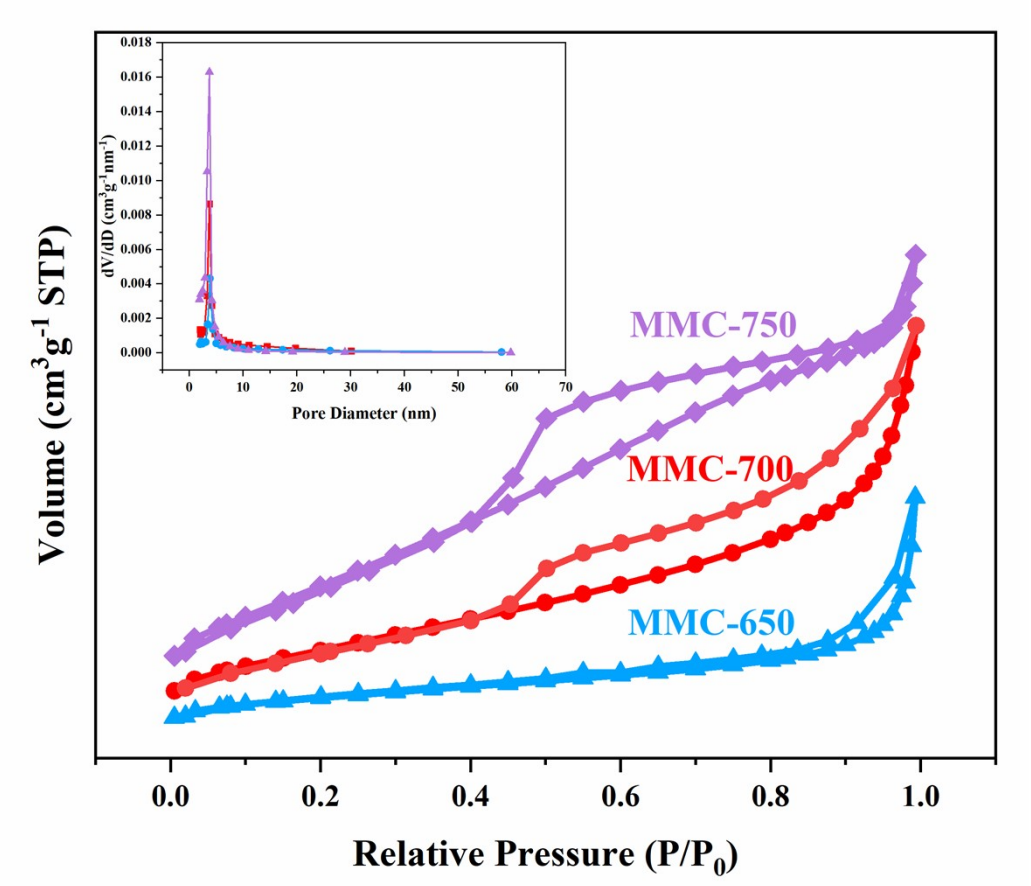

Figure S2. N_2 adsorption-desorption isotherms (inset: pore size distribution).

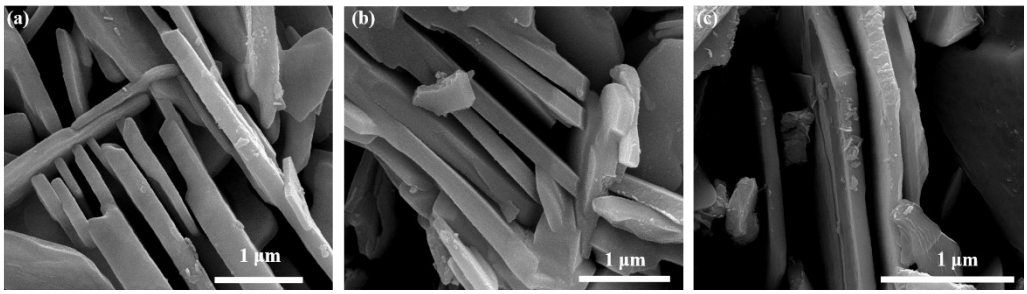

Figure S3. SEM images of (a) MMC-650, (b) MMC-700, (c) MMC-750.

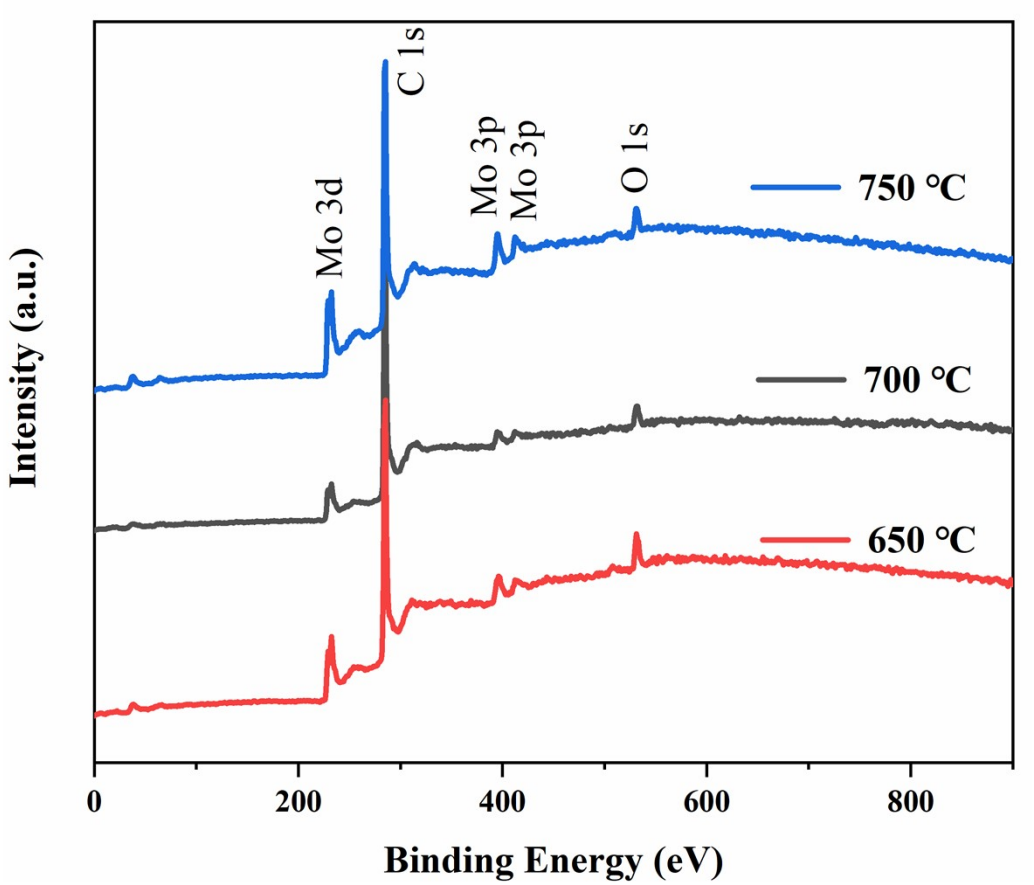

Figure S4. The wide XPS spectra of MMC-650, MMC-700 and MMC-750.

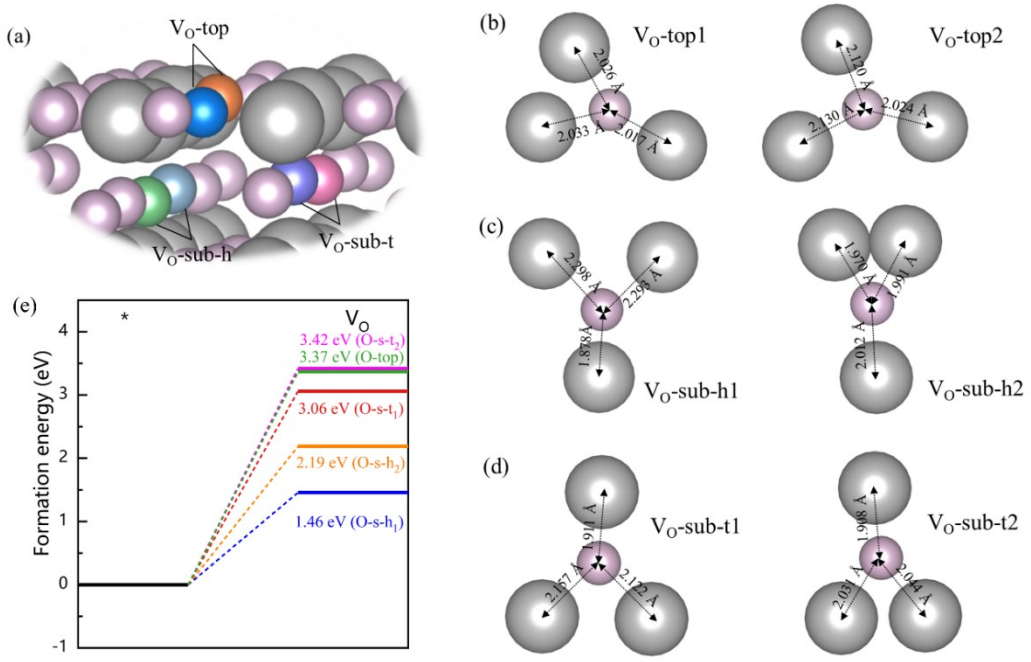

Figure S5. Six types of O atoms in the MoO_2 (011) surface. (a) Diagram of six types of O atoms, and the spheres marked with different colors represent six different

O atoms. (b)-(d) The coordination environment of O atoms and the bond lengths of Mo-O. To facilitate the discussion, the structures were renumbered as V_O-top$_n$, V_O-sub-h$_n$ and V_O-sub-t$_n$ (n = 1,2). The grey and purple spheres represent Mo and O atoms, respectively. (e) Formation energies of six types of O vacancy.

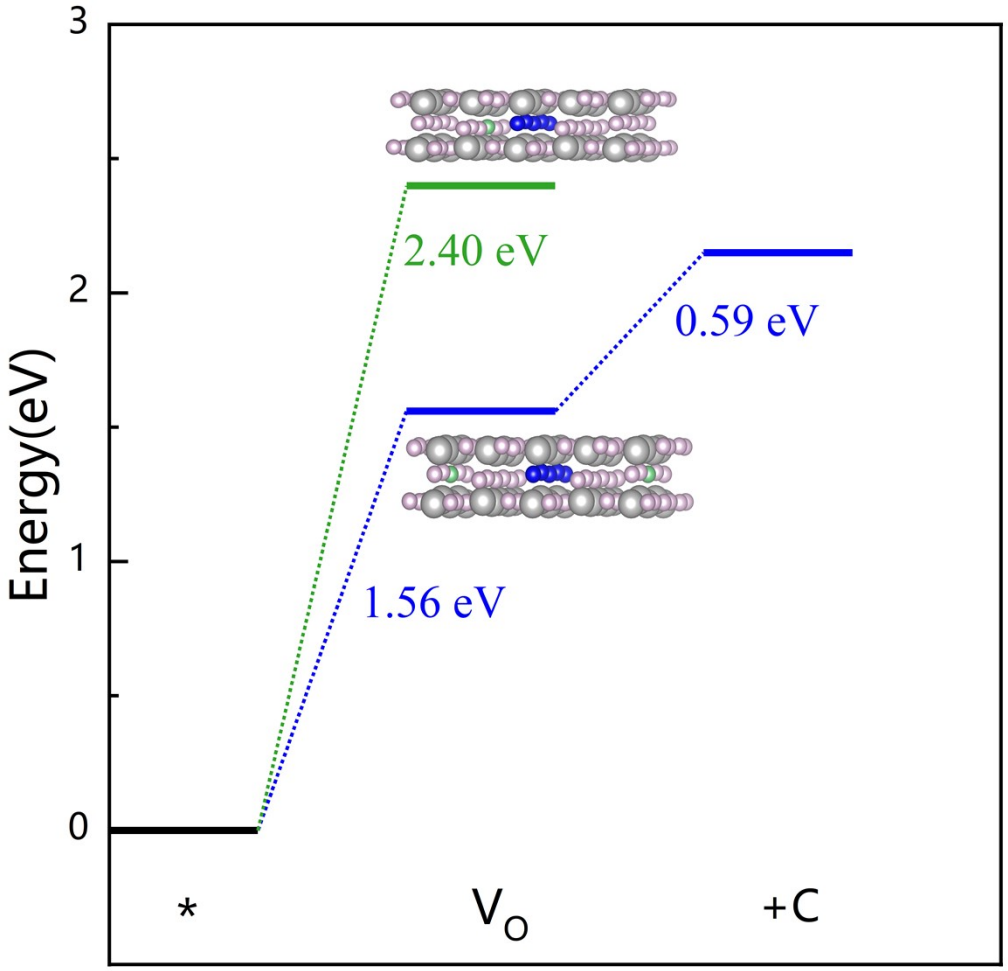

Figure S6. The minimum energy paths of the substitution reaction in the second round. The insets show the V_O (green spheres) configuration. Blue, green, grey and purple spheres represent C, O vacancies, Mo and O atoms, respectively.

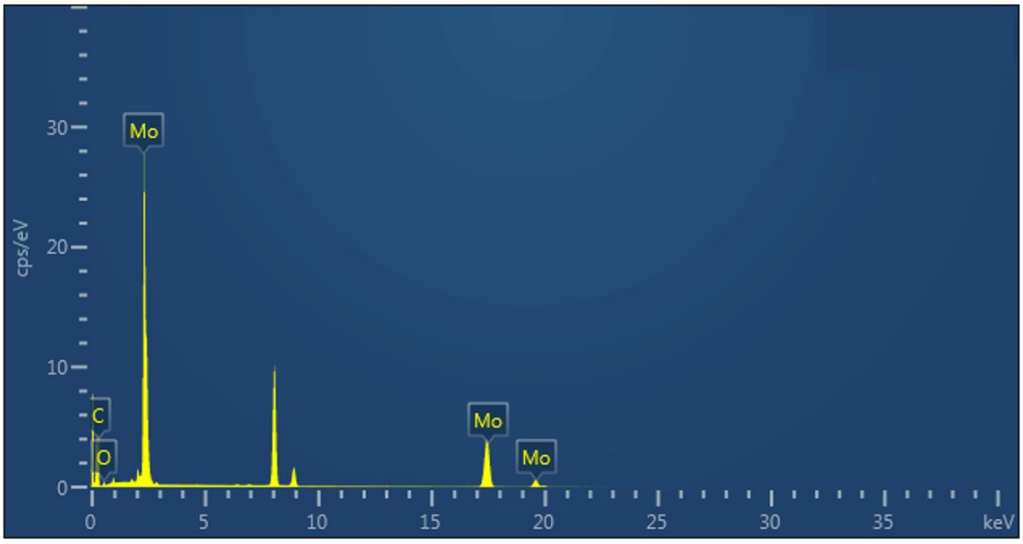

Figure S7. EDS spectrum of MMC-700.

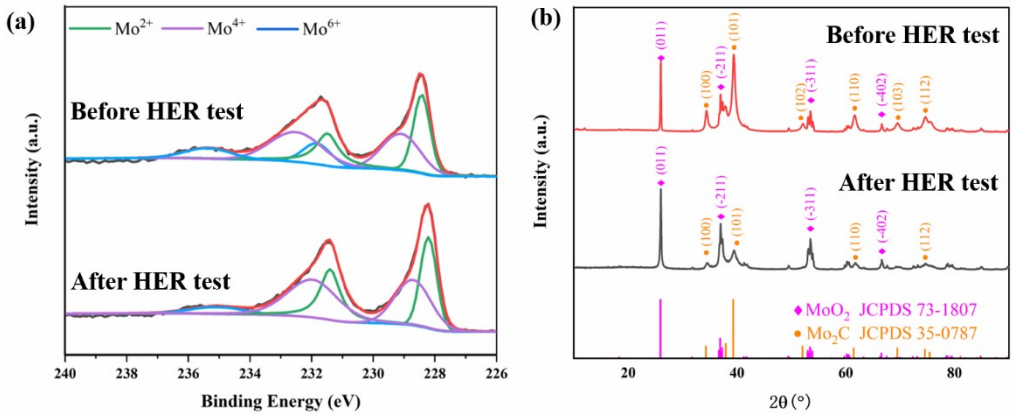

Figure S8. (a) XPS spectrum of Mo 3d before and after HER test. (b) XRD result of MMC-700 before and after HER test.

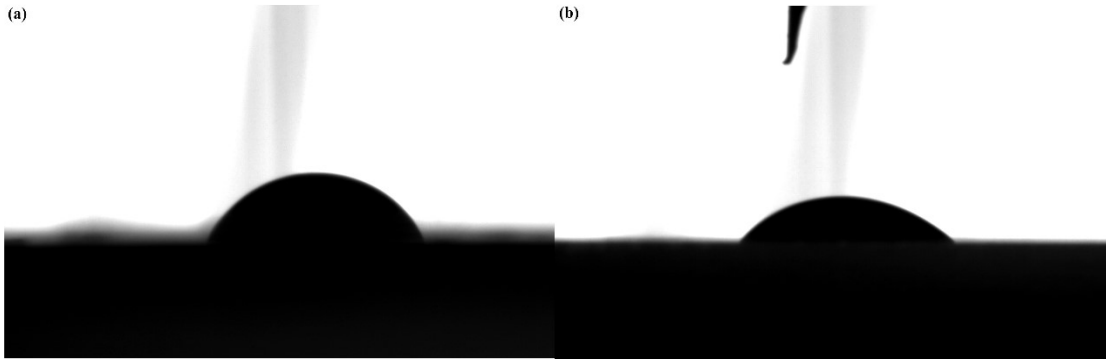

Figure S9. (a) Contact angle test image of MoO_3. (b) Contact angle test image of MoO_2-Mo_2C@C.

Table S1. The mass percentage and atomic percentage of elements of MMC-700 according to the EDS elemental mapping results.

Element	Line type	K factor	Wt.%	At.%
C	K-line system	2.742	10.15	46.58
O	K-line system	2.001	0.64	2.19
Mo	K-line system	4.910	89.21	51.23

Table S2. Comparison of the required overpotentials (η) in obtaining the current density of 10 mA/cm^2 and the electrochemically double layer capacitance (C_{dl}) with recently reported Mo_2C-based HER catalysts in 0.5 M H_2SO_4.

Catalysts	Overpotential (mV@10 mA cm^{-2})	C_{dl} (mF cm^{-2})	Ref.
NP-Mo_2C	210	29.4	[1]
NS-Mo_2C	223	5.8	[1]
Ni/β-Mo_2C	192	1.52	[2]
Mo_2C@Graphitic Carbon	151	32	[3]
Co/α-Mo_2C	196	40	[4]
MoC/Mo_2C-690	159	28.25	[5]
Mo_2C/C	180	10..9	[6]
Mo_2C/VC@C	122	3.8	[7]
VN/Mo_2C	140	45	[8]
N-Mo_2C@NC	136	12.01	[9]
MoO_2-Mo_2C@C	**176**	**50.7**	**This work**

Table S3. Comparison of the required overpotentials (η) in obtaining the current density of 10 mA/cm^2 and the electrochemically double layer capacitance (C_{dl}) with recently reported Mo_2C-based HER catalysts in 1 M KOH.

Catalysts	Overpotential (mV@10 mA cm^{-2})	Tafel slope (mV dec^{-1})	Ref.

Ni/β-Mo_2C	157	86	[2]
MoC-Mo_2C-690	132	40.2	[5]
Mo_2C@NPC	72	15.1	[10]
Mo_2C/C	210	23.1	[6]
CoP/Mo_2C-NC	103	90	[11]
Sn-Mo_2C@C	144	38.56	[12]
β-Mo_2C@C	146	35.6	[13]
MoS_2-Mo_2C	109	99	[14]
Co, Mo_2C-CNF	128	108.9	[15]
Ni-Mo_2C/NCNFs	143	29.41	[16]
MoO_2-Mo_2C@C	**129**	**60.1**	**This work**

References

1. D. Wang, T. Liu, J. Wang and Z. Wu, *Carbon*, 2018, **139**, 845-852.
2. T. Ouyang, A. N. Chen, Z. Z. He, Z. Q. Liu and Y. Tong, *Chem. Commun.*, 2018, **54**, 9901-9904.
3. J. Zhu, Y. Yao, Z. Chen, A. Zhang, M. Zhou, J. Guo, W. D. Wu, X. D. Chen, Y. Li and Z. Wu, *ACS Appl. Mater. Interfaces*, 2018, **10**, 18761-18770.
4. A. M. Gómez–Marín and E. A. Ticianelli, *Appl. Catal., B*, 2017, **209**, 600-610.
5. W. Liu, X. Wang, F. Wang, K. Du, Z. Zhang, Y. Guo, H. Yin and D. Wang, *Nat. Commun.*, 2021, **12**, 6776.
6. D. Wang, J. Wang, X. Luo, Z. Wu and L. Ye, *ACS Sustainable Chem. Eng.*, 2017, **6**, 983-990.
7. C. Huang, X. Miao, C. Pi, B. Gao, X. Zhang, P. Qin, K. Huo, X. Peng and P. K. Chu, *Nano Energy*, 2019, **60**, 520-526.
8. L. Feng, S. Li, D. He, L. Cao, G. Li, P. Guo and J. Huang, *ACS Sustainable Chem. Eng.*, 2021, **9**, 15202-15211.
9. Q. Jing, J. Zhu, X. Wei, Y. Lin, X. Wang and Z. Wu, *J. Colloid Interface Sci.*, 2021, **602**, 520-533.
10. C. Lu, D. Tranca, J. Zhang, F. N. Rodri Guez Hernandez, Y. Su, X. Zhuang, F. Zhang, G. Seifert and X. Feng, *ACS Nano*, 2017, **11**, 3933-3942.
11. T. Liu, S. Zhou, J. Qi, K. Wang, L. Zheng, Q. Huang, T. Zhou and J. Zhang, *J. Energy Chem.*, 2021, **58**, 370-376.
12. L. Zhang, K. Wei, J. Ma, J. Wang, Z. Liu, R. Xing and T. Jiao, *Appl. Surf. Sci.*, 2021, **566**, 150754.
13. Q. Yan, X. Yang, T. Wei, C. Zhou, W. Wu, L. Zeng, R. Zhu, K. Cheng, K. Ye, K. Zhu, J. Yan, D. Cao and G. Wang, *J. Colloid Interface Sci.*, 2020, **563**, 104-111.
14. Z. Zhao, F. Qin, S. Kasiraju, L. Xie, M. K. Alam, S. Chen, D. Wang, Z. Ren, Z. Wang, L. C. Grabow and J. Bao, *ACS Catal.*, 2017, **7**, 7312-7318.
15. J. Wang, R. Zhu, J. Cheng, Y. Song, M. Mao, F. Chen and Y. Cheng, *Chem. Eng. J.*, 2020, **397**, 125481.
16. M. Li, Y. Zhu, H. Wang, C. Wang, N. Pinna and X. Lu, *Adv. Energy Mater.*, 2019, **9**, 1803185.